International Journal of Medical Physics, Clinical Engineering and Radiation Oncology, 2026, 15(2), 41-52
https://www.scirp.org/journal/ijmpcero
ISSN Online: 2168-5444
ISSN Print: 2168-5436

Feasibility Study of Measuring the Dose Per Pulse and Instantaneous Dose Rates Using a Silicon Photodiode Detector for a 10-MV Flattening Filter-Free Mode in Radiation Therapy

Satoshi Yamaguchi

Department of Electrical and Electronic Engineering, Faculty of Engineering, Hokkaido University of Science, Sapporo, Japan
Email: yamaguchi-s@hus.ac.jp

How to cite this paper: Yamaguchi, S. (2026) Feasibility Study of Measuring the Dose Per Pulse and Instantaneous Dose Rates Using a Silicon Photodiode Detector for a 10-MV Flattening Filter-Free Mode in Radiation Therapy. *International Journal of Medical Physics, Clinical Engineering and Radiation Oncology*, **15**, 41-52.
https://doi.org/10.4236/ijmpcero.2026.152004

Received: April 7, 2026
Accepted: May 8, 2026
Published: May 11, 2026

Abstract

This study aimed at developing a pulse dosimeter for radiation therapy. The dose per pulse (DPP) and instantaneous dose rates of a commercially available medical linear accelerator were measured using a novel detector composed of a silicon photodiode (Si-PD) with a 0.4-mm-thick Cu filter, single operational amplifier, resistor, capacitor, and substrate. The pulse voltages from the detector were measured using an analog-to-digital converter. The dependence of 50, 100, 150, 200, and 250 monitor units (MU) was measured at a depth of 100 mm with a field size of 100 × 100 mm^2 and a constant distance of 1.0 m between the source and detector. Each MU was subjected to three measurements under a 10-MV flattening filter-free mode with a dose rate of 2400 MU/min. The DPP (mGy) was calibrated at 100 MUs using a Farmer-type ionization chamber, and the instantaneous dose rates were calculated using assumed values of a 2.8 ms pulse interval and a 4.5 μs pulse width. The depth dependence was also measured at 20 and 100 mm with a field size of 50 × 50 mm^2 for 100 MUs. The number of pulses was proportional to that of MUs with maximum values of DPP being 1.422 and 1.100 mGy/pulse at depths of 20 and 100 mm, respectively; the corresponding instantaneous dose rates were 0.508 and 0.393 Gy/s at 2.8 ms and 316.0 and 244.3 Gy/s at 4.5 μs. The results indicate that the developed Si-PD detector can efficiently measure DPP and instantaneous dose rates.

Keywords

Silicon Photodiode, Dosimetry, Dose Per Pulse, Radiotherapy, Instantaneous

Dose Rate

1. Introduction

The primary purpose of various types of dosimeters used in radiotherapy is to ensure that the cumulative absorbed dose in patients planned by the treatment planning system. However, there exists a trade-off between damage to normal tissues and therapeutic effect, which limits the prescribed dose. An ultra-high dose-rate radiation therapy, referred to as "FLASH", has been gaining attention owing to its sparing effect on normal tissue without compromising the therapeutic effect on the tumor [1]. Several studies have reported the effectiveness of FLASH in small animals [2]-[4], and the development of a clinical treatment device using X-rays, electron beams, and proton beams has been investigated [5] [6]. However, the mechanism underlying the effects remains unclear.

Recently, the flattening filter-free (FFF) mode has been introduced in medical LINACs, enabling substantially higher dose rates by removing the flattening filter [7]-[9]. Although its biological effects appear comparable to those of conventional radiotherapy [10] [11], to date, no commercially available dosimeter has been reported that is validated for the direct measurement of dose rate or dose per pulse (DPP) in FFF beams. To assess potential FLASH-related effects, it is essential to account for dose-rate variations in conventional treatments, particularly through accurate measurement of DPP.

Therefore, I propose a pulse detector to measure the DPP using a silicon photodiode (Si-PD) as a relative dosimeter in this study. The Si-PD sensor (with sensitive dimensions of 1.3×1.3 mm^2) is smaller than the smallest ionization chamber, providing a simple and cost-effective electrical circuit design. Additionally, the circuit can be applied to multi-dimensional array detectors as it uses a voltage of less than 5.0 V.

The Si-PD sensor has been used to measure the cumulative dose for the development of capacitor dosimeters [12] [13]. Therein, I developed a cumulative dosimeter using a Si-PD with a capacitor to measure the cumulative dose using a medical LINAC; the calibrated dose was in good agreement with the value measured using a commercially available ionization chamber with a small standard deviation [14] [15].

Subsequently, I developed a Si-PD detector for measuring dose rates using a resistor of 20 MΩ with a time constant of 2.0 ms [16]. The detector could measure up to 0.61 Gy/s using a customized X-ray tube generator, and the dose rate was proportional in the range of 0.05 to 0.6 Gy/s. However, the number of pulses (pulse count) could not be adequately detected using a medical LINAC because the measured pulse width was large owing to the time constant. Moreover, the analog-to-digital converter (ADC) used was inadequate in its performance.

Based on these findings, I propose a novel Si-PD pulse detector in this study,

wherein a high-speed ADC is used and the resistance is modified from 20 MΩ to 2 MΩ. Herein, I investigated the monitor unit (MU) and depth dependencies of the developed Si-PD pulse detector. A 10-MV FFF mode with a dose rate of 2400 MU/min was used for measurements to output the maximum dose rate in a commercially available medical LINAC.

At present, there is no standardized dose-rate dosimeter available for radiotherapy. Therefore, I used a Farmer-type ionization chamber to convert the DPP and provisionally calculated the instantaneous dose rates.

2. Methods

Figure 1(a) depicts the configuration of the Si-PD pulse detector. Figure 1(b) illustrates the appearance and electrical circuit of the substrate. The Si-PD substrate comprises a Si-PD sensor (S1087-01; Hamamatsu Photonics KK), complementary metal-oxide semiconductor (CMOS) single operational amplifier (LMC6081; Texas Instruments), resistor (2 MΩ; KOA), and capacitor (100 pF; TDK). The Si-PD sensor was shaded using a 75-μm-thick aluminum tape and covered with a Cu filter of 0.4 mm thickness for energy correction. A 2.5-mm-thick acrylic plate was attached below the substrate for insulation. Additionally, three dry cell batteries of 1.5 V were used to power the CMOS single operational amplifier at approximately 4.5 V. The Si-PD sensor with sensitive dimensions of 1.3×1.3 mm^2 detected ionizing radiation as photocurrents, which were converted into output voltages using the single operational amplifier in the substrate. The amplified output voltages were then converted into digital data using a high-speed ADC (RAI-16, ELMOS Co., Ltd.) with a sampling period of 0.1 ms (sampling clock = 10 kHz) via a lead wire. The measured data were stored on a personal computer (PC) through a universal serial bus (USB) cable. The Si-PD pulse detector output a

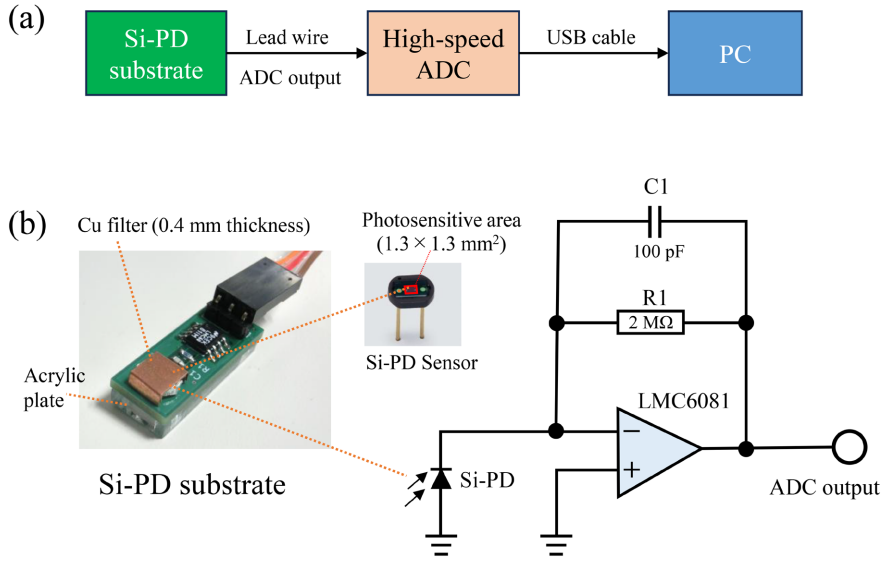

Figure 1. Configuration of the silicon photodiode (Si-PD) pulse detector. (b) Appearance and electrical circuit of the Si-PD sensor with a 0.4-mm-thick Cu filter, single operational amplifier, resistor, capacitor, and substrate.

pulse waveform as the voltage, and the peak voltages of the pulse is proportional to the DPP. Therefore, the peak voltages were extracted and used for the DPP conversion.

Figure 2 depicts the experimental setup used for measurements with a medical LINAC (TrueBeamSTx, Varian Medical Systems) and a solid-water phantom (WD, Kyoto Kagaku, Japan) with a physical density of 1020 kg m^{-3}. The upper surface of the Si-PD sensor was set to a constant distance of 1000 mm from the X-ray source. The depth was set to 100 mm by placing the sensor in the solid-water phantom. The source-to-surface distance (SSD) was 900 mm and the field size was 100 × 100 mm^2 at a distance of 1000 mm on a medical LINAC. The 10-MV FFF mode with a dose rate of 2400 MU/min and outputs of 50, 100, 150, 200, and 250 MUs was employed. These measurements were performed three times for each MU using a Si-PD substrate, and the peak voltages were extracted. The pulse peak voltages were extracted using an Excel macro that compared three consecutive data points in the measured time-series. A data point was identified as a local peak when its value exceeded those of the preceding and following points. To avoid noise-related false detections, only peaks with amplitudes greater than 0.05 V were recognized as valid pulses, and their peak voltages were recorded. The collected data were statistically analyzed using JMP 10 software (SAS Institute Inc.) based on the one-way analysis of variance (ANOVA). The differences among averages were analyzed using a two-sided student's t-test, with the level of statistical significance set to $p < 0.05$.

As the number of measured peak voltages is identical to the pulse count, the MU dependence of the pulse count was also evaluated.

DPP conversion was performed with an output of 100 MUs and a depth of 100 mm, based on an absolute dose measured using a Farmer-type ionization chamber

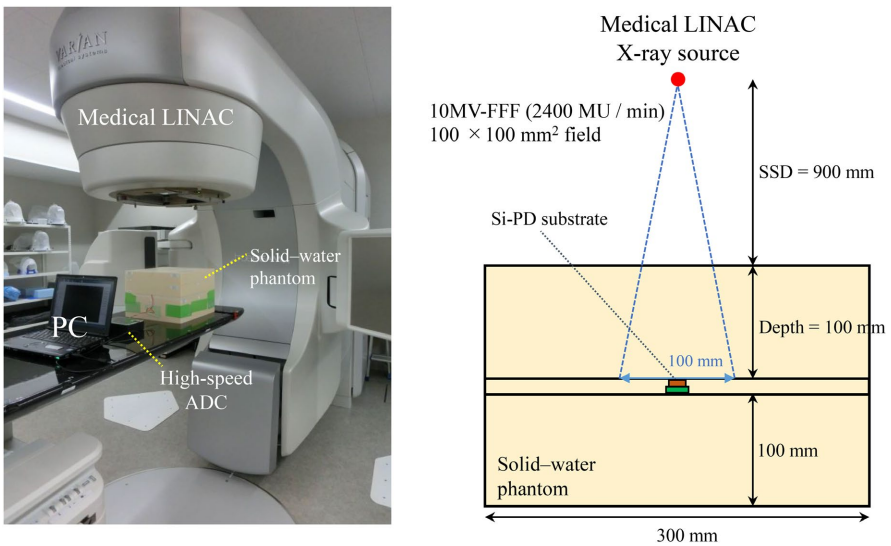

Figure 2. Experimental setup for pulse measurement using a medical linear accelerator (LINAC) with a field size of 100 × 100 mm^2 and source-to-surface distance (SSD) of 900 mm.

(N30013; PTW, Freiburg) at a position identical to that of the Si-PD substrate. The conversion factor (*CF*) was calculated using the following equation:

$$CF\left(\frac{\text{mGy}}{V}\right)=\frac{D_a\left(\text{mGy}\right)}{V_s\left(V\right)}$$

where D_a denotes the absolute dose (mGy) and V_s indicates the sum of the peak voltages (V) measured using the Si-PD pulse detector. *CF* was used to convert the peak voltages (V) into DPP (mGy) and calculate the instantaneous dose rates by considering a pulse interval time of 2.8 ms and a pulse width of 4.5 μs in the medical LINAC (Varian Medical Systems, personal communiqué).

Furthermore, the depth dependence was evaluated using a solid-water phantom. The upper surface of the Si-PD sensor was set to a constant value of 1000 mm from the X-ray source, and depths of 20 and 100 mm were measured in the solid-water phantom, with SSDs of 980 and 900 mm, respectively. A field size of 50 × 50 mm^2 at a distance of 1000 mm and 10-MV FFF mode with a dose rate of 2400 MU/min at 100 MUs were used. The measurement was performed once and the peak voltages were extracted for each depth.

3. Results

Figure 3 illustrates the output voltages measured at a depth of 100 mm with a field size of 100 × 100 mm^2 using a Si-PD pulse detector. Figures 3(a)-(c) depict the 1st, 2nd, and 3rd measurement results with irradiation starting from 0 to 140 ms, respectively. The pulse waveforms appeared clearly for each measurement, and variations in the peak voltage, indicative of DPP, were observed. The pulse interval was approximately 2.8 ms under all conditions. However, some missing

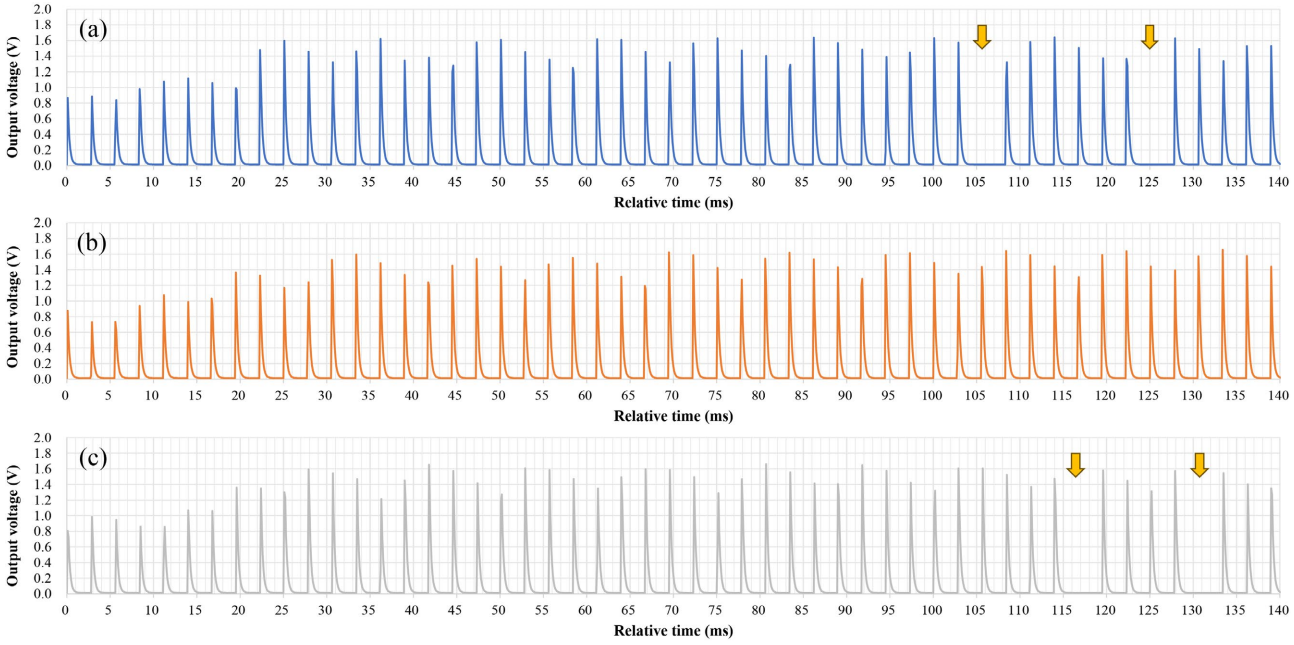

Figure 3. Measurement of pulse voltages using a silicon photodiode (Si-PD) pulse detector at a depth of 100 mm with a field size of 100 × 100 mm^2 at a source-to-surface distance (SSD) of 900 mm.

pulses were observed (indicated by arrows in Figure 3(a) and Figure 3(c)). Additionally, significantly low peak voltages of less than 1.0 V were observed from the initiation of irradiation up to approximately several tens of milliseconds under all conditions.

Table 1 lists the pulse counts obtained from the peak voltages extracted for each condition. The difference in the pulse counts for each MU was within three pulses.

Figure 4 depicts the relationship between the MU and average pulse counts. The measured pulse counts were proportional to the number of MUs.

Table 1. Number of pulses extracted from the peak voltages measured using a Si-PD pulse detector. Measurements were performed three times for each MU.

MU	Number of pulses			Average ± SD
	1st	2nd	3rd	
50	409	408	408	408.3 ± 0.58
100	810	811	810	810.3 ± 0.58
150	1213	1213	1213	1213.0 ± 0.00
200	1615	1617	1616	1616.0 ± 1.00
250	2018	2016	2015	2016.3 ± 1.53

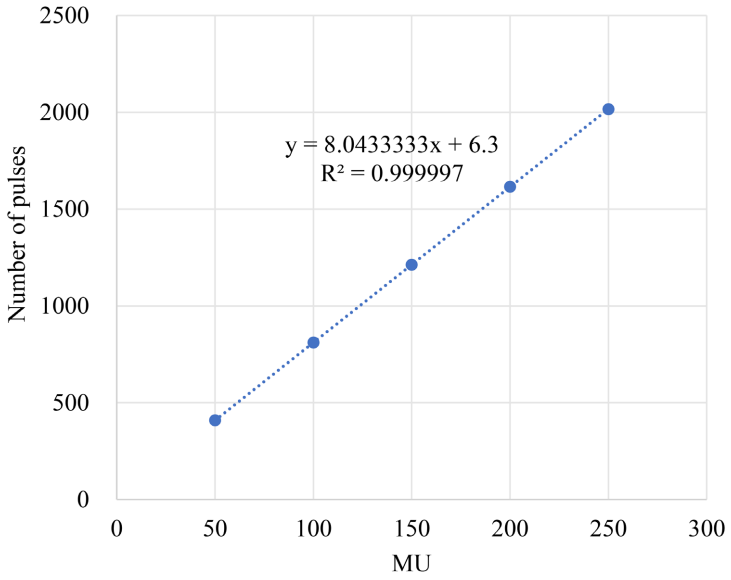

Figure 4. Monitor unit (MU) dependence evaluated using a silicon photodiode (Si-PD) pulse detector. The linear approximation was calculated using JMP 10 software ($p < 0.0001$*)

Table 2 lists the peak voltages extracted under each condition. The average and standard deviation (SD) are presented in Table 2(a), and the sum of the peak voltages is summarized in Table 2(b). Those extracted peak voltages include the low-amplitude pulses observed during the first several tens of milliseconds under each condition. A comparison of the peak voltages using ANOVA was determined

to be statistically significant for 200 and 250 MUs at $p = 0.0009$ and 0.0002, respectively. The value of *Vs* at 100 MUs was 1221.7 V.

Figure 5 illustrates a statistical comparison of the peak voltages for each MU using a two-sided student's t-test with a significance level of $p < 0.05$. These boxplots indicate medians, average values (cross marks), outliers, maximum values, minimum values, and 25th and 75th percentiles. The results were statistically insignificant for 50 MUs (Figure 5(a)) and 100 MUs (Figure 5(b)), whereas the results exhibited some statistical significance for 150 MUs (Figure 5(c)), 200 MUs (Figure 5(d)) and 250 MUs (Figure 5(e)). The outliers were observed under all conditions.

Figure 6 depicts the calibration results for DPP. The absolute dose (*Da*) measured using the ionization chamber was 0.8064 Gy for 100 MUs; therefore, the

Table 2. (a) Average values and standard deviation (SD) of peak voltages and statistical comparison obtained using ANOVA. (b) Sum of the peak voltages and *Vs* (average of the sum of the peak voltages).

MU	(a) Average ± SD of peak voltage (V)			*p* value	(b) Sum of peak voltage (V)			Average (*Vs*)
	1st	2nd	3rd		1st	2nd	3rd	
50	1.490 ± 0.141	1.490 ± 0.140	1.488 ± 0.138	0.9765	609.6	607.9	607.3	608.3
100	1.512 ± 0.127	1.507 ± 0.131	1.505 ± 0.128	0.5454	1224.3	1221.9	1218.8	1221.7
150	1.531 ± 0.124	1.520 ± 0.124	1.520 ± 0.127	0.0650	1856.7	1844.3	1844.2	1848.4
200	1.552 ± 0.123	1.544 ± 0.122	1.535 ± 0.123	0.0009*	2505.9	2496.1	2481.2	2494.4
250	1.575 ± 0.122	1.570 ± 0.122	1.559 ± 0.121	0.0002*	3178.0	3164.6	3141.9	3161.5

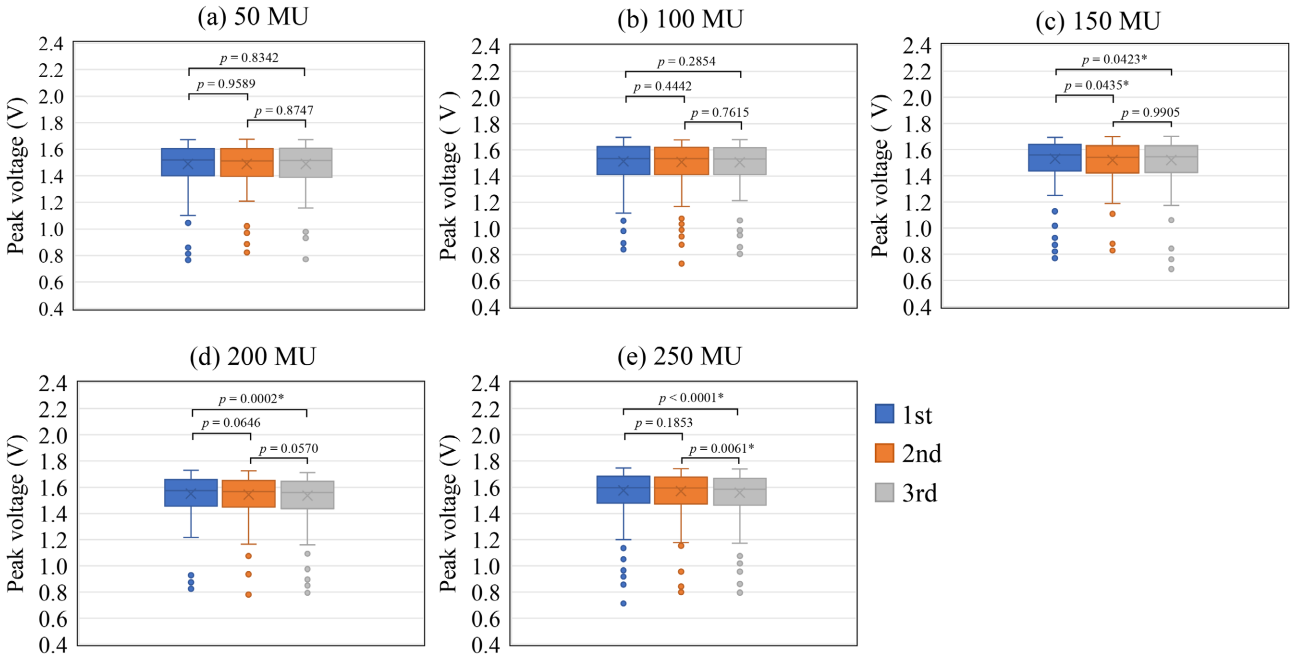

Figure 5. Statistical comparison of the peak voltages extracted from the output voltages for the dependence of 50, 100, 150, 200, and 250 monitor units (MUs) performed using the student's t-test at a significance level of $p < 0.05$. The boxplots indicate medians, average values (cross marks), outliers, maximum values, minimum values, and 25th and 75th percentiles.

value of *CF* was 0.660 mGy/V. Figure 6(a) shows the DPP calibration results multiplied by the extracted peak voltages and *CF* values. Figure 6(b) and Figure 6(c) illustrate the instantaneous dose rates calculated by considering a pulse interval of 2.8 ms and a pulse width of 4.5 μs. The maximum DPP was 1.120 mGy/pulse, and the instantaneous dose rates were 0.400 Gy/s at 2.8 ms and 248.9 Gy/s at 4.5 μs.

Figure 7 depicts the results of depth dependence using a field size of 50 × 50 mm^2 at depths of 20 and 100 mm. The output voltages were measured once at each depth using a Si-PD pulse detector. The difference in the extracted peak voltages was observed, and the DPP at 20 mm was higher than that at 100 mm. The maximum

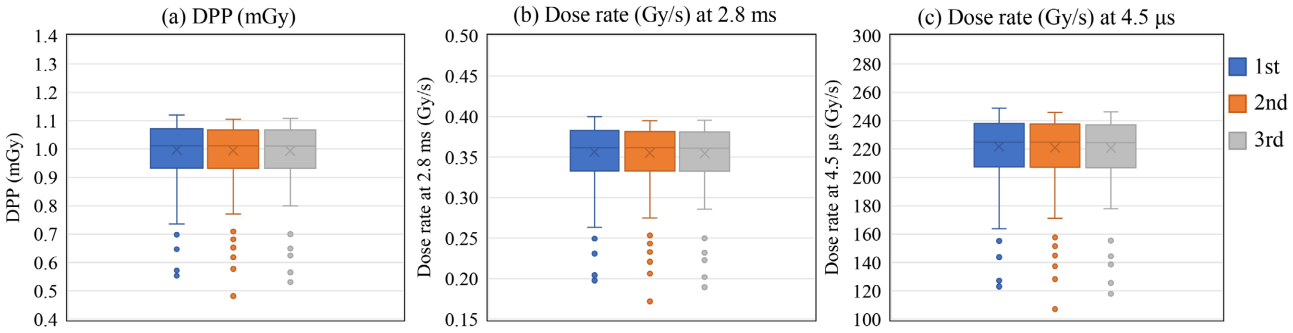

Figure 6. Dose calibration results of the silicon photodiode (Si-PD) pulse detector with a field size of 100 × 100 mm^2 and a depth of 100 mm. (a) Dose per pulse. (b) Dose rate at 2.8 ms (pulse interval). (c) Dose rate at 4.5 μs (pulse width). The boxplots include medians, average values (cross marks), outliers, maximum values, minimum values, and 25th and 75th percentiles

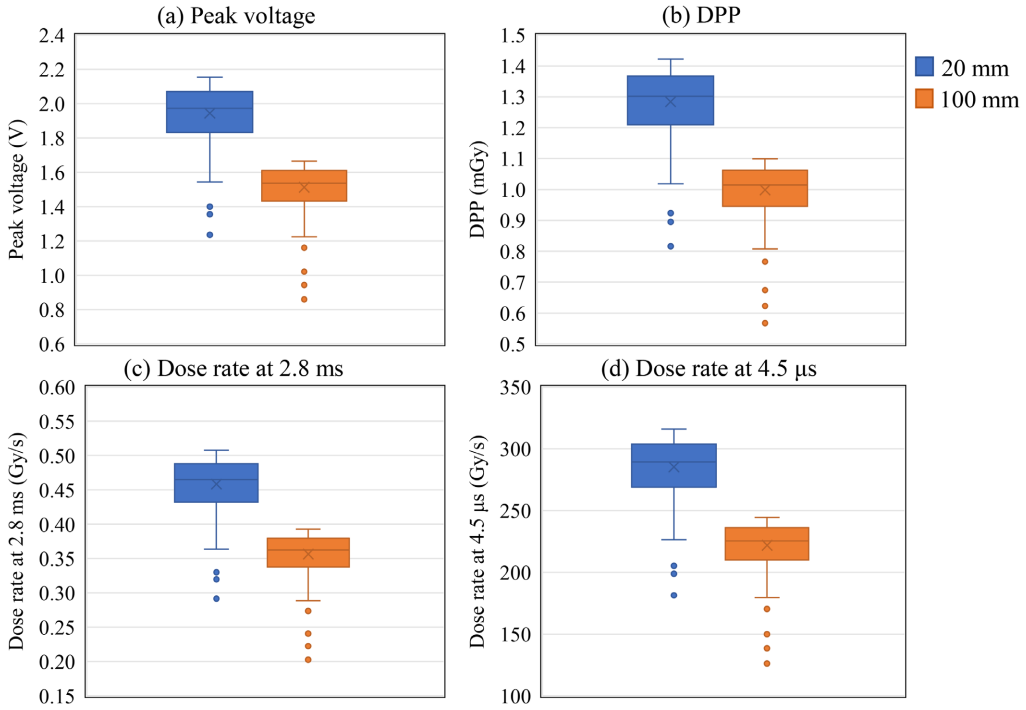

Figure 7. Depth dependence for a field size of 50 × 50 mm^2 in the 10-MV flattening filter-free (FFF) mode. (a) Peak voltage. (b) Dose per pulse. (c) Dose rate at 2.8 ms (pulse interval). (d) Dose rate at 4.5 μs (pulse width). The boxplots include medians, average values (cross marks), outliers, maximum values, minimum values, and 25th and 75th percentiles.

DPP values at depths of 20 and 100 mm were 1.422 and 1.100 mGy/pulse, respectively. The maximum instantaneous dose rates at depths of 20 and 100 mm were 0.508 and 0.393 Gy/s at 2.8 ms and 316.0 and 244.3 Gy/s at 4.5 μs, respectively.

4. Discussion

The FFF mode comprises a function called dose servo, which achieves the average dose rate by reducing the pulse during irradiation [17]. The pulse losses in the pulse waveforms (**Figure 3(a)** and **Figure 3(c)**) were attributed to dose servo. However, the difference of only a few pulses measured three times at each MU (**Table 1**) was observed with high reproducibility.

A statistically significant difference was observed in the peak voltages as the number of MUs increased (**Figure 5**). These observations suggest that when the MU value is high, the reproducibility of the output decreases due to variations in the DPP parameter.

As no standardized method exists for measuring DPP, I calculated the radiation dose using an ionization chamber, which is used as a standard dosimeter in radiation therapy. The absorbed dose (Gy) of water calculated by the ionization chamber was the cumulative dose; this was converted to DPP by calculating the sum of each peak voltage and by determining the value of *CF*. This calculation method is feasible because the FFF mode uses a constant pulse width. However, the calibration method used in this study is a simplified approach derived from the cumulative dose. Because it includes the low-amplitude pulses observed during the first several tens of milliseconds, it is not suitable as a future DPP calibration method.

Regarding the depth dependence, measurements with the ionization chamber at a depth of 20 mm were subject to large uncertainties because this region lies within the buildup region and is therefore unsuitable as a calibration condition. For this reason, a depth of 100 mm with a standard field size of 100 × 100 mm^2 was adopted as the calibration condition. A detailed investigation of the depth dependence of the *CF* value for the Si-PD pulse detector used in this study was not conducted and remains a subject for future work.

Furthermore, because the pulse detector used in this study has a time constant of 0.2 ms, the measured pulse width is broadened. Therefore, the true pulse width on the order of several microseconds cannot be directly determined.

To obtain more accurate DPP and dose-rate values with this detector, an appropriate calibration procedure using a high-accuracy reference dosimeter capable of pulse measurements must be established. In this study, provisional DPP and dose rates were calculated from the measured peak voltages; however, the pulse interval of 2.8 ms and the pulse width of 4.5 μs used for the dose-rate calculation were estimated values based on various sources. The measurement and validation of the pulse width and pulse interval were also not addressed in this work and remain subjects for future investigation.

As a reference, several studies have reported DPP measurements in FFF mode. Xiao *et al.* [18] reported a DPP value of 0.13 cGy/pulse (*i.e.*, 1.3 mGy/pulse) at a

depth of 2.3 cm (dmax) in a 10-MV FFF beam based on the manufacturer's information; this corresponds to the median value shown in Figure 7(b) at a depth of 20 mm.

This study confirmed the feasibility of measuring pulsed photon beams generated in the flattening filter free (FFF) mode of a medical linear accelerator using a Si PD pulse detector. The measurement and characterization of other types of ionizing radiation remain subjects for future investigation.

5. Conclusion

In this study, I developed a novel detector for pulse measurement using a Si-PD sensor and investigated the feasibility of DPP measurement in the 10-MV FFF mode using a commercially available medical LINAC. The pulse waveform measured by the detector exhibited reduced pulses during the irradiation because of the dose servo function of the FFF mode, and a significantly low DPP was observed for several tens of milliseconds after the initiation of irradiation. However, the overall difference was of only a few pulses with high reproducibility. The number of pulses measured was proportional to that of MUs. Both DPP and instantaneous dose rates were provisionally calculated using an ionization chamber, and the results were equivalent to those obtained in the FFF mode. The results confirm that the Si-PD pulse detector can be a promising tool for measuring DPP and instantaneous dose rates in radiation therapy.

Acknowledgements

I would like to express our sincere gratitude to Honorary Professor Eiichi Sato for his significant contribution to the design principles of the dose-rate dosimeter. I also thank Mr. Nobuaki Mega for his assistance with the experiments. Part of this work was conducted at Iwate Medical University Hospital, Iwate Medical University. I am grateful to Professors Hisanori Ariga and Kunihiro Yoshioka for kindly providing access to the research facilities. I thank Editage (https://www.editage.com/) for English language editing. This work was supported by JSPS KAKENHI (Grant number 22K07644).

Conflicts of Interest

The author declares no conflicts of interest regarding the publication of this paper.

References

[1] Hughes, J.R. and Parsons, J.L. (2020) FLASH Radiotherapy: Current Knowledge and Future Insights Using Proton-Beam Therapy. *International Journal of Molecular Sciences*, **21**, Article 6492. https://doi.org/10.3390/ijms21186492

[2] Gao, F., Yang, Y., Zhu, H., Wang, J., Xiao, D., Zhou, Z., *et al.* (2022) First Demonstration of the FLASH Effect with Ultrahigh Dose Rate High-Energy X-Rays. *Radiotherapy and Oncology*, **166**, 44-50. https://doi.org/10.1016/j.radonc.2021.11.004

[3] Zhu, H., Xie, D., Wang, Y., Huang, R., Chen, X., Yang, Y., *et al.* (2023) Comparison

of Intratumor and Local Immune Response between MV X-Ray FLASH and Conventional Radiotherapies. *Clinical and Translational Radiation Oncology*, **38**, 138-146. https://doi.org/10.1016/j.ctro.2022.11.005

[4] Zhu, H., Xie, D., Yang, Y., Huang, S., Gao, X., Peng, Y., *et al.* (2022) Radioprotective Effect of X-Ray Abdominal FLASH Irradiation: Adaptation to Oxidative Damage and Inflammatory Response May Be Benefiting Factors. *Medical Physics*, **49**, 4812-4822. https://doi.org/10.1002/mp.15680

[5] Schulte, R., Johnstone, C., Boucher, S., Esarey, E., Geddes, C.G.R., Kravchenko, M., *et al.* (2023) Transformative Technology for FLASH Radiation Therapy. *Applied Sciences*, **13**, Article 5021. https://doi.org/10.3390/app13085021

[6] Jolly, S., Owen, H., Schippers, M. and Welsch, C. (2020) Technical Challenges for FLASH Proton Therapy. *Physica Medica*, **78**, 71-82. https://doi.org/10.1016/j.ejmp.2020.08.005

[7] Georg, D., Knöös, T. and McClean, B. (2011) Current Status and Future Perspective of Flattening Filter Free Photon Beams. *Medical Physics*, **38**, 1280-1293. https://doi.org/10.1118/1.3554643

[8] Ma, C., Chen, M., Long, T., Parsons, D., Gu, X., Jiang, S., *et al.* (2019) Flattening Filter Free in Intensity-Modulated Radiotherapy (IMRT)—Theoretical Modeling with Delivery Efficiency Analysis. *Medical Physics*, **46**, 34-44. https://doi.org/10.1002/mp.13267

[9] Pokhrel, D., Halfman, M. and Sanford, L. (2020) FFF-VMAT for SBRT of Lung Lesions: Improves Dose Coverage at Tumor-Lung Interface Compared to Flattened Beams. *Journal of Applied Clinical Medical Physics*, **21**, 26-35. https://doi.org/10.1002/acm2.12764

[10] Verbakel, W.F.A.R., van den Berg, J., Slotman, B.J. and Sminia, P. (2013) Comparable Cell Survival between High Dose Rate Flattening Filter Free and Conventional Dose Rate Irradiation. *Acta Oncologica*, **52**, 652-657. https://doi.org/10.3109/0284186x.2012.737021

[11] Nakano, H., Minami, K., Yagi, M., Imaizumi, H., Otani, Y., Inoue, S., *et al.* (2018) Radiobiological Effects of Flattening Filter-Free Photon Beams on A549 Non-Small-Cell Lung Cancer Cells. *Journal of Radiation Research*, **59**, 442-445. https://doi.org/10.1093/jrr/rry041

[12] Yamaguchi, S. and Sato, E. (2019) Product Development of a Condenser Dosimeter Using a Skin-Insulated USB-A-Substrate with a Silicon X-Ray Diode. *Radiological Physics and Technology*, **12**, 69-75. https://doi.org/10.1007/s12194-018-00493-4

[13] Yamaguchi, S., Ieko, Y., Ariga, H. and Yoshioka, K. (2021) Characterization of an Under-Development Capacitor Dosimeter Equipped with a Silicon X-Ray Diode. *Review of Scientific Instruments*, **92**, Article 123101. https://doi.org/10.1063/5.0061061

[14] Yamaguchi, S., Sato, E., Ieko, Y., Ariga, H. and Yoshioka, K. (2020) A Capacitor Dosimeter with Disposable Silicon-Diode Substrates for 4-MV X-Ray Beam Detection in Radiation Therapy. *Physics Open*, **4**, Article 100026. https://doi.org/10.1016/j.physo.2020.100026

[15] Yamaguchi, S., Ieko, Y., Ariga, H. and Yoshioka, K. (2023) Electron Beam Detection in Radiotherapy Using a Capacitor Dosimeter Equipped with a Silicon Photodiode. *Medical & Biological Engineering & Computing*, **61**, 2197-2205. https://doi.org/10.1007/s11517-023-02870-7

[16] Yamaguchi, S., Ariga, H. and Yoshioka, K. (2024) Development of a Dose-Rate Dosimeter Using a Silicon Photodiode for a Medical Linear Accelerator in a 10 MV Flat-

tening Filter-Free Mode. *Review of Scientific Instruments*, **95**, Article 053102. https://doi.org/10.1063/5.0179656

[17] Kry, S.F., Popple, R., Molineu, A. and Followill, D.S. (2012) Ion Recombination Correction Factors (Pion) for Varian TrueBeam High-Dose-Rate Therapy Beams. *Journal of Applied Clinical Medical Physics*, **13**, 318-325. https://doi.org/10.1120/jacmp.v13i6.3803

[18] Xiao, Y., Kry, S.F., Popple, R., Yorke, E., Papanikolaou, N., Stathakis, S., *et al.* (2015) Flattening Filter-Free Accelerators: A Report from the AAPM Therapy Emerging Technology Assessment Work Group. *Journal of Applied Clinical Medical Physics*, **16**, 12-29. https://doi.org/10.1120/jacmp.v16i3.5219